

# Chiral Conflict among Different Helicenes Suppresses Formation of One Enantiomorph in 2D Crystallization

Johannes Seibel,<sup>†</sup> Oliver Allemann,<sup>‡</sup> Jay S. Siegel,<sup>‡</sup> and Karl-Heinz Ernst<sup>\*,†,‡</sup>

<sup>†</sup>Empa, Swiss Federal Laboratories for Materials Science and Technology, 8600 Dübendorf, Switzerland

<sup>‡</sup>Department of Chemistry, University of Zurich, 8057 Zürich, Switzerland

**S** Supporting Information

**ABSTRACT:** Diastereomeric interactions in 2D crystals formed at solid surfaces serve as excellent models for understanding molecular recognition in biomineralization. Adsorption of a pentahelicene racemate on a Au(111) surface leads to 2D conglomerate crystallization, i.e., homochiral mirror domains, as observed by scanning tunneling microscopy. Upon mixing 26% of (*M*)-heptahelicene into the racemate monolayer, only the (*M*)-pentahelicene enantiomorph is observed. This effect is explained by a preferred heterochiral interaction between the different helicene species, suppressing the formation of the pure (*P*)-pentahelicene enantiomorph. These results shine new light onto stereoselective molecular recognition mediated by van der Waals forces.

Cooperativity and selectivity among chiral biomolecules is of fundamental importance to life. Such stereochemical recognition plays an especially important role in homochiral imperative of molecular evolution.<sup>1</sup> Furthermore, such chiral molecular recognition plays a key role in phenomena like spontaneous resolution in crystallization of enantiomers, enantioseparation via diastereomeric salt crystallization, and the performance of liquid crystal devices. The co-operative nature of these phenomena render them more difficult to understand; extremely small structural influences govern the macroscopic result when they become amplified by many co-operating units. Investigation of complexity often benefits the study of appropriate model systems—in the present context, two-dimensional (2D) crystallization of monolayers comprising chiral molecules on single-crystal surfaces.<sup>2–4</sup>

Molecular recognition among “helicenes”,<sup>5</sup> in particular, ortho-annulated,  $\pi$ -conjugated carbohelicenes, may affect the use of their outstanding material and chiroptical properties in device applications. In the case of surfaces, the 2D crystallization of heptahelicene ([7]H, C<sub>30</sub>H<sub>18</sub>, Figure 1), [11]anthrahelicene, hexathia[11]helicene, and their derivatives shows stereoselective polymorph behavior.<sup>6–18</sup> On Cu(111) [7]H forms heterochiral 2D crystals,<sup>19</sup> whereas the polar 6,13-dicyano derivative undergoes lateral separation into a 2D conglomerate of homochiral domains.<sup>20</sup> Self-assembly of 5-amino[6]helicene at the Au(111)/liquid interface resulted in co-existence of a 2D conglomerate and a racemic phase.<sup>21</sup> These results support early predictions of spontaneous resolution in Langmuir–Blodgett films, stating that heterochiral recognition is favored for van der Waals interactions and that

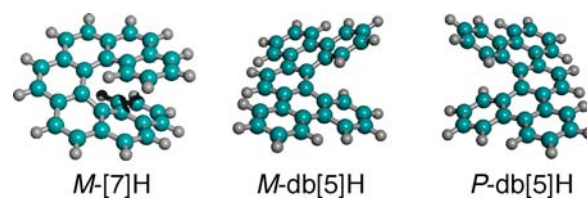


**Figure 1.** Ball-and-stick molecular models for the C<sub>30</sub>H<sub>18</sub> isomers *M*-[7]H, *M*-db[5]H, and *P*-db[5]H.

polar forces favor homochiral recognition.<sup>22</sup> Theory also predicts that in closed-packed systems, when repulsion becomes significant, homochiral or heterochiral discrimination is more pronounced due to an increased influence of molecular shape or symmetry.<sup>23</sup> However, no spontaneous 2D resolution into a conglomerate for non-functionalized helicenes has been reported so far.

A common technique to achieve optical resolution of enantiomers is diastereomeric salt crystallization, a method established in 1893 by Pope and Kipping,<sup>24</sup> and separation of enantiomers via crystallization is still the most important means for obtaining enantiopure compounds.<sup>25</sup> Pasteur in 1853 reported quasi-racemate formation for the co-crystallization of tartaric acid (TA) and malic acid (MA).<sup>26</sup> On Cu(110), racemic TA usually forms a 2D conglomerate,<sup>27</sup> but (*S,S*)-tartrate prefers a quasiracemic mixture with (*R*)-MA and leaves (*R,R*)-TA unaffected, so only a single enantiomorph was observed.<sup>28</sup> Basically the same effect has been observed for TA at enantiomeric excess (*ee*) of  $\geq 0.2$  on Cu(110).<sup>29</sup> In both cases, a chiral conflict is induced, either by an enantiomer of a different species or by excess of one enantiomer, disturbing the homochiral crystallization of the minority handedness by forming a quasiracemic mixture or an unbalanced solid solution. Preferred hydrogen bonding in the mixture has been cited as a possible underlying cause for this phenomenon.<sup>28</sup> Diastereomeric selectivity at the solid–liquid interface has recently been reported for acid–base interactions.<sup>30</sup> Consequently, one may ask whether nonpolar helicenes induce a similar effect.

This study focuses on the spontaneous resolution of [5,6,9,10]-dibenzopentahelicene (db[5]H, C<sub>30</sub>H<sub>18</sub>, Figure 1) on a gold(111) surface. That is, only homochiral mirror domains are observed in the close-packed monolayer via scanning tunneling microscopy (STM) after deposition of *rac*-db[5]H. The

Received: March 12, 2013

Published: May 2, 2013

homochiral composition is concluded here from STM with submolecular resolution, clearly revealing the identical sense of helicity for every molecule in a single-crystalline domain. Mixing small amounts of *M*-[7]H into the monolayer then suppresses formation of the *P*-db[5]H enantiomorph, and only the *M*-db[5]H enantiomorph is observed.

Racemic [7]H was purchased from Chiracon GmbH. Metal substrate preparation and enantioseparation of [7]H have been described previously.<sup>13</sup> Racemic db[5]H was synthesized from difluoroquinquephenyl by intramolecular Friedel–Crafts-type arylation, using silylium-ion-promoted C–F bond activation.<sup>31</sup> Difluoroquinquephenyl was derived from 1-fluoro-2-bromobenzene by two consecutive Negishi cross couplings with 1-bromo-2-iodobenzene and 1,4-diiodobenzene, respectively (Supporting Information). The helicenes were deposited by sublimation *in vacuo* from a cell held at 170 °C (db[5]H) and 160 °C (*M*-[7]H). The Au(111) substrate was kept at room temperature during deposition, at which the molecules were too mobile to form ordered structures. After deposition of different amounts of *M*-[7]H, db[5]H was added until a coverage of a complete monolayer was reached. In layers prepared with lower coverages, the mobility of the molecules at 50 K was still too high to observe ordered structures. The sample was then slowly cooled to allow 2D crystallization. All STM images were taken under ultra-high-vacuum conditions ( $p < 5 \times 10^{-10}$  mbar) with a commercial variable-temperature scanning tunneling microscope (Omicron Nanotechnology) at temperatures around 50 K. In the mixing experiments, we give the ratios as area covered by the species: 20% of *M*-[7]H corresponds to one-fifth of the saturated *M*-[7]H layer and roughly 26% of the total number of molecules at the surfaces when mixed with racemic db[5]H.

Figure 2 shows STM images of db[5]H on Au(111). Different domains of ordered crystallites are embedded in areas with low degree of order. Some domains can be superimposed by rotation by 120°, marked in Figure 2a by identical color, but others need to be reflected for superposition (Figure 2a, different color). The angle between these mirror domains is 24° (Figure 2b). Short-range STM images reveal that a single domain consists of molecules of identical handedness (Figure 2c,d). Different heights within a molecule are represented by brightness. In a constant-current STM image, the contrast of a single molecule (Figure 2c, inset) is dominated by a bright protrusion, marking the upper ring in the molecule. Following decreasing brightness gives a clockwise or counterclockwise descent (marked with lobes colored in a red-blue-green-yellow sequence in Figures 2c,d) and thus the sense of helicity. Domains colored in blue consist of *M*-db[5]H, and those colored in yellow consist of *P*-db[5]H. This example shows that polar functional groups and directed interactions are not required in order to achieve 2D conglomerate crystallization of all-carbon helicenes at surfaces.

One feature of the homochiral domains is that molecules partly overlap (Figure 3). That is, the upper terminal ring of helix I is located in part above the third ring of helix II. A similar packing motif has been reported for helical subunits of hexabenzocoronene on Cu(111).<sup>32</sup> One can think of similar close-packing for heterochiral dimers, but these do not fit into the observed unit cell nor allow buildup of an extended layer (Supporting Information Figure S1). Consequently, the homochiral arrangement arises due to denser packing. A 2×3 unit cell configuration is shown in Supporting Information Figure S2. We assume that favored adsorption sites for db[5]H

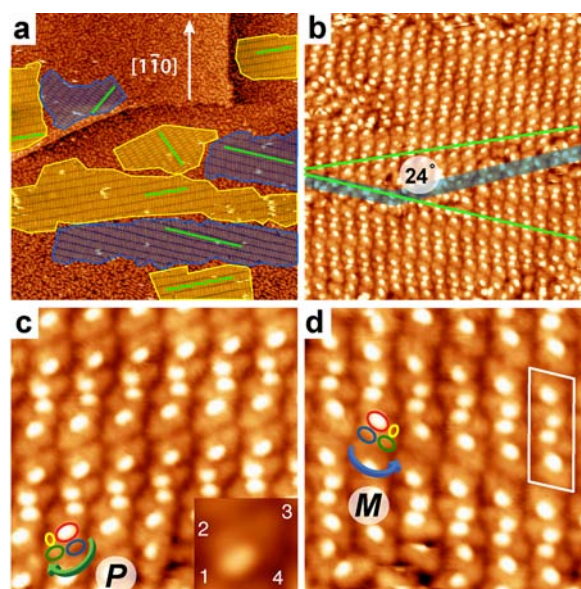


**Figure 2.** STM images of db[5]H on Au(111). (a) Large area scan (150 nm × 150 nm,  $U = -2.725$  V,  $I = 25$  pA) showing co-existence of crystalline and disordered areas. Opposite mirror domains are marked in blue and yellow. (b) STM image (30 nm × 30 nm,  $U = 2.051$  V,  $I = 28$  pA) showing two mirror domains and their shared boundary (semitransparent blue line). Each domain is tilted by 12° with respect to a defined direction given by the substrate. (c,d) 10 nm × 10 nm images of both domains ( $U = 2.051$  V,  $I = 28$  pA). The sense of helicity is deduced from the submolecular resolution. Going from high to low brightness (red-blue-green-yellow lobes), the absolute helicity is determined, indicated here by colored arrows, with the tips pointing to the lower ends closer to the surface. Going from 1 to 4 (panel c inset, 2 nm × 2 nm, same as panel c, but enlarged 30 times) also clearly reveals the *P*-helix. A single unit cell contains four molecules. In all images the  $[1\bar{1}0]$  crystal orientation points up, as indicated in panel a. The lengths of the unit cell vectors are 1.52 and 3.74 nm, the latter being identical with the distance between the bright stripes.

on the metallic surface grid contribute to the chiral discrimination, but we are unable to identify them. The motivation to use the dibenzo derivative instead of plain pentahelicene was to have a lower mobility in order to be able to observe ordered structures at 50 K. We anticipate that up to three aromatic rings—two terminal rings of the helix and one benzo group—are oriented parallel to the surface.

The portion of disordered area is substantial. Apparently the mobility at nucleation and growth was too low (cooling rate to fast) to allow the mass transport needed. The disorder itself is then due to unbalanced mixtures because of the vicinity of an enantiopure domain. Recall that 9% of *P*-[7]H was sufficient to eliminate order in the *M*-[7]H monolayer.<sup>19</sup> For the heterochiral arrangement of *rac*-[7]H on Cu(111), a much better degree of order has been established, but no mass transport was required there.<sup>11</sup> The balance between *M*- and *P*-db[5]H domains seemed to be shifted already at a coverage of 10% of *M*-[7]H in the layer (Supporting Information Figure S3). At 20% *M*-[7]H, only *M*-db[5]H domains are left as ordered structures (Figure 4). The degree of disorder increases when *M*-[7]H is mixed into the *rac*-db[5]H. With all *P*-domains disappeared, less than 10% of the surface is covered on average with ordered *M*-db[5]H domains (Supporting Information Figure S4). The average *M*-domain size drops to about half the size observed for the pure *rac*-db[5]H layer (Supporting Information Table S1). This supports again the scenario that an

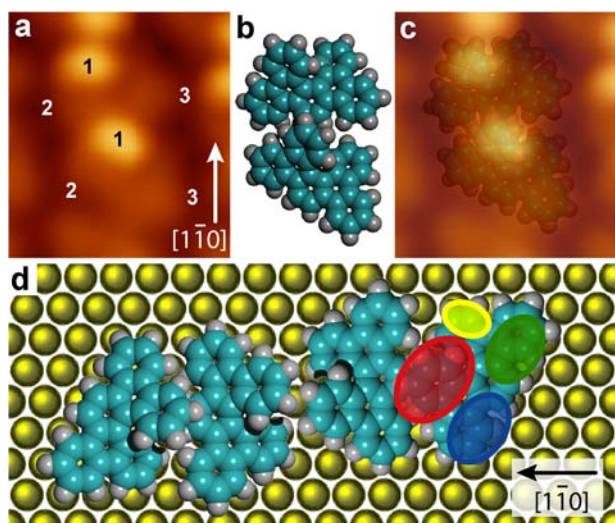


**Figure 3.** Superposition of an STM image (a,  $U = 2.051$  V,  $I = 28$  pA, 30 times enlarged) and a model of the homochiral db[5]H dimer (b) shows partly overlapping molecules (c). The handedness of the partly covered molecule is identical to the one above, as indicated by the sequence of three lobes with decreasing intensity (a). The two molecules are rotated by  $45^\circ$  with respect to each other. The arrangement of the molecules in the unit cell (d) is the result of a more extended superposition of model and STM image (Supporting Information Figure S1).

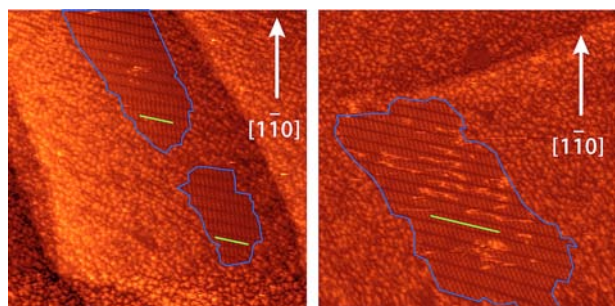


**Figure 4.** STM images ( $100$  nm  $\times$   $100$  nm,  $U = -2.725$  V,  $I = 31$  and  $66$  pA) of a monolayer covered with  $80\%$  *rac*-db[5]H and  $20\%$  *M*-[7]H. Only the *M*-db[5]H enantiomorph can be observed.

enantiomeric unbalanced layer suppresses ordered structures. Beyond the competition between racemic crystal and conglomerate formation, an additional chiral conflict is induced.

The interaction of different chiral species at surfaces has led to the discovery of intriguing co-operative effects, similar to the “sergeant-and-soldiers” or “majority-rule” experiments in polymer science. Small chiral bias, stemming from side chains in helical polyisocyanate co-polymers, induced single helicity.<sup>33,34</sup> In a 2D sergeant-and-soldiers experiment, single-handed enantiomorphism in chiral monolayers of prochiral succinic acid and *meso*-TA was induced by doping with (*R,R*)- or (*S,S*)-TA on Cu(110).<sup>35,36</sup> The prochiral molecules turn chiral at the surface, presumably by forming a zigzag-distorted adsorbate,<sup>37</sup> and form 2D conglomerates.<sup>38,39</sup> The small chiral bias introduced by chiral TA, however, is sufficient to switch all prochiral species into single handedness, which is defined by the zigzag of the chiral TA enantiomer.<sup>40</sup> Such chiral amplification, but rather based on small *ee*, has also been shown for [7]H on Cu(111).<sup>11</sup> The chiral entity there was a heterochiral pair with two possible enantiomorphous align-

ments. Chiral bias from *ee* caused the single sense of enantiomorphism on the entire surface.

In contrast to these amplification mechanisms, the present study deals with a chiral conflict between different species. The imbalance of opposite domains changes therefore gradually with increasing *M*-[7]H content (Supporting Information Figure S4). In these helicene mixtures apparently *M*-[7]H captures preferably *P*-db[5]H into the disordered area. However, it also breaks up in part the *M*-domains. Due to the lack of polar groups, the diastereomeric interaction has to be of van der Waals type, and the larger the overlap between molecules, the stronger the pair formation. The best overlap is found for a heterochiral diastereomer (Supporting Information Figure S5). At a first glance, such a mechanism does not include any co-operativity, but a differently aligned diastereomeric pair induces disorder in the surrounding layer, increasing the effect of enantiomorph suppression. Only the majority with the right handedness then has a chance to nucleate under these conditions. The effect of selective suppression might be less pronounced here due to the fact that the unfavored enantiomer cannot disappear from the surface as observed, for example, at the liquid–solid interface.<sup>30</sup>

These results show that polar forces, like previously observed for Pasteur’s quasiracemate or for TA at excess on Cu(110),<sup>28,29</sup> are not required in order to suppress a single enantiomorph. It is rather the balance between homochiral and heterochiral interactions. A remarkable enantiospecific interaction has previously been reported for adenine and phenylglycine co-adsorbed on Cu(110).<sup>41</sup> The selective diastereomer formation was explained by substrate-mediated charge transfer and Coulomb repulsion between the amino groups of both species.<sup>42</sup> For polar species on Cu(110) the surface may indeed play an important role in chiral recognition. Chiral reconstructions of Cu(110) have been observed for MA<sup>43,44</sup> and TA<sup>45</sup> with STM. However, these helicenes studies exclude any surface mechanism beyond the fact that certain surface binding sites might be favored. The intermolecular lateral recognition should be purely van der Waals.

In conclusion, these studies show that apolar pentahelicenes crystallize into a conglomerate of homochiral 2D domains on a gold surface, which is in contrast to previous work performed on heptahelicene on Cu(111). Mixing with enantiopure heptahelicene leads to suppression of one pentahelicene enantiomorph, an effect that has only been observed so far for polar tartaric acid on Cu(110). Concerning chiral discrimination, this work shows that dispersive forces at surfaces can act in a manner comparable to polar forces.

## ■ ASSOCIATED CONTENT

### 📄 Supporting Information

STM images, db[5]H synthesis, db[5]H unit cell model structures for homo- and heterochiral content, quantitative analysis of ordered areas, and *M*-to-*P* domain area ratios with increasing *M*-[7]H content as well as models for diastereomeric pairs. This material is available free of charge via the Internet at <http://pubs.acs.org>.

## ■ AUTHOR INFORMATION

### Corresponding Author

karl-heinz.ernst@empa.ch

### Notes

The authors declare no competing financial interest.

## ■ ACKNOWLEDGMENTS

This work was supported by the Swiss National Science Foundation, project "Supramolecular Chiral Films".

## ■ REFERENCES

- (1) Siegel, J. S. *Chirality* **1998**, *10*, 24–27.
- (2) Ernst, K.-H. *Phys. Status Solidi B* **2012**, *249*, 2057–2088.
- (3) Pérez-García, L.; Amabilino, D. B. *Chem. Soc. Rev.* **2007**, *36*, 941–967.
- (4) Katsonis, N.; Lacaze, E.; Feringa, B. L. *Mater. Chem.* **2008**, *18*, 2065–2073.
- (5) Shen, Y.; Chen, C.-F. *Chem. Rev.* **2012**, *112*, 1463–1535.
- (6) Ernst, K.-H.; Böhringer, M.; McFadden, C. F.; Hug, P.; Müller, U.; Ellerbeck, U. *Nanotechnology* **1999**, *10*, 355–361.
- (7) Ernst, K.-H.; Kuster, Y.; Fasel, R.; McFadden, C. F.; Ellerbeck, U. *Surf. Sci.* **2003**, *530*, 195–202.
- (8) Fasel, R.; Cossy, A.; Ernst, K.-H.; Baumberger, F.; Greber, T.; Osterwalder, J. J. *Chem. Phys.* **2001**, *115*, 1020–1027.
- (9) Ernst, K.-H.; Neuber, M.; Grunze, M.; Ellerbeck, U. *J. Am. Chem. Soc.* **2001**, *123*, 493–495.
- (10) Fasel, R.; Parschau, M.; Ernst, K.-H. *Angew. Chem., Int. Ed.* **2003**, *42*, 5178–5181.
- (11) Fasel, R.; Parschau, M.; Ernst, K.-H. *Nature* **2006**, *439*, 449–452.
- (12) Parschau, M.; Ellerbeck, U.; Ernst, K.-H. *Colloids Surf., A* **2010**, *354*, 240–245.
- (13) Ernst, K.-H.; Kuster, Y.; Fasel, R.; Müller, M.; Ellerbeck, U. *Chirality* **2001**, *13*, 675–678.
- (14) Stöhr, M.; Boz, S.; Schär, M.; Nguyen, M.-T.; Pignedoli, C. A.; Passerone, D.; Schweizer, W. B.; Thilgen, C.; Jung, T. A.; Diederich, F. *Angew. Chem., Int. Ed.* **2011**, *50*, 9982–9986.
- (15) Rahe, P.; Nimmrich, M.; Greuling, A.; Schütte, J.; Stará, I. G.; Rybáček, J.; Huerta-Angeles, G.; Starý, I.; Rohlfing, M.; Kühnle, A. J. *Phys. Chem. C* **2010**, *114*, 1547–1552.
- (16) Rybáček, J.; Huerta-Angeles, G.; Kollárovič, A.; Stará, I. G.; Starý, I.; Rahe, P.; Nimmrich, M.; Kühnle, A. *Eur. J. Org. Chem.* **2011**, 853–860.
- (17) Godlewski, S.; Prauzner-Bechcicki, J. S.; Budzioch, J.; Walczak, L.; Stará, I. G.; G.; Starý, I.; Sehnal, P.; Szymonski, M. *Surf. Sci.* **2012**, *606*, 1600–1607.
- (18) Taniguchi, M.; Nakagawa, H.; Yamagishi, A.; Yamada, K. *J. Mol. Catal. A: Chem.* **2003**, *199*, 65–71.
- (19) Parschau, M.; Fasel, R.; Ernst, K.-H. *Cryst. Growth Des.* **2008**, *8*, 1890–1896.
- (20) Hauke, C. M.; Rahe, P.; Nimmrich, M.; Schütte, J.; Stará, I. G.; Rybáček, J.; Huerta-Angeles, G.; Starý, I.; Rohlfink, M.; Kühnle, A. J. *Phys. Chem. C* **2012**, *116*, 4637–4641.
- (21) Balandina, T.; van der Meijden, M. W.; Ivasenko, O.; Cornil, D.; Cornil, J.; Lazzaroni, R.; Kellog, R. M.; De Feyter, S. *Chem. Commun.* **2013**, *49*, 2207–2209.
- (22) Andelman, J. *J. Am. Chem. Soc.* **1989**, *111*, 6536–6544.
- (23) Schipper, P. E.; Harrowell, P. R. *J. Am. Chem. Soc.* **1983**, *105*, 723–730.
- (24) Kipping, F. S.; Pope, W. J. *J. Chem. Soc. Trans.* **1893**, *63*, 548–604.
- (25) Sheldon, R. A. *Chiral Technologies: Industrial synthesis of optically active compounds*; Marcel Dekker: New York, 1993.
- (26) Pasteur, L. *Ann. Chim. Phys.* **1853**, *38*, 437–483.
- (27) Romer, S.; Behzadi, B.; Fasel, R.; Ernst, K.-H. *Chem.–Eur. J.* **2005**, *11*, 4149–4154.
- (28) Roth, C.; Passerone, D.; Ernst, K.-H. *Chem. Commun.* **2010**, *46*, 8645–8647.
- (29) Haq, S.; Liu, N.; Humblot, V.; Jansen, A. P. J.; Raval, R. *Nat. Chem.* **2009**, *1*, 409–414.
- (30) Xu, H.; Saletta, W. J.; Iavicoli, P.; Van Aeverbeke, B.; Ghijssens, E.; Mali, K. S.; Schenning, A. P. H. J.; Beljonne, D.; Lazzaroni, R.; Amabilino, D. B.; De Feyter, S. *Angew. Chem., Int. Ed.* **2012**, *51*, 11981–11985.
- (31) Allemann, O.; Duttwyler, S.; Baldrige, K. K.; Siegel, J. S. *Science* **2011**, *332*, 574–577.
- (32) Treier, M.; Ruffieux, P.; Groning, P.; Xiao, S. X.; Nuckolls, C.; Fasel, R. *Chem. Commun.* **2008**, 4555–4557.
- (33) Green, M. M.; Reidy, M. P.; Johnson, R. J.; Darling, G.; O’Leary, D. J.; Wilson, G. *J. Am. Chem. Soc.* **1989**, *111*, 6452–6454.
- (34) Green, M. M.; Garetz, B. A.; Munoz, B.; Chang, H.; Hoke, S.; Cooks, R. G. *J. Am. Chem. Soc.* **1995**, *117*, 4181–4182.
- (35) Parschau, M.; Behzadi, B.; Romer, S.; Ernst, K.-H. *J. Am. Chem. Soc.* **2004**, *126*, 15398–15399.
- (36) Parschau, M.; Kampen, T.; Ernst, K.-H. *Chem. Phys. Lett.* **2005**, *407*, 433–437.
- (37) Barbosa, L. A. M. M.; Sautet, P. *J. Am. Chem. Soc.* **2001**, *123*, 6639–6648.
- (38) Humblot, V.; Ortega Lorenzo, M.; Baddeley, C. J.; Haq, S.; Raval, R. *J. Am. Chem. Soc.* **2004**, *126*, 6460–6469.
- (39) Parschau, M.; Behzadi, B.; Romer, S.; Ernst, K.-H. *Surf. Interface Anal.* **2006**, *38*, 1607–1610.
- (40) Fasel, R.; Wider, J.; Quitmann, C.; Ernst, K.-H.; Greber, T. *Angew. Chem., Int. Ed.* **2004**, *43*, 2853–2856.
- (41) Chen, Q.; Richardson, N. V. *Nat. Mater.* **2003**, *2*, 324–328.
- (42) Blankenburg, S.; Schmidt, W. G. *Phys. Rev. Lett.* **2007**, *99*, 196107/1–4.
- (43) Roth, C.; Parschau, M.; Ernst, K.-H. *ChemPhysChem* **2011**, *12*, 1572–1577.
- (44) Roth, C.; Passerone, D.; Merz, L.; Parschau, M.; Ernst, K.-H. *J. Phys. Chem. C* **2011**, *115*, 1240–1247.
- (45) Mhatre, B.; Pushkarev, V. V.; Holsclaw, B.; Lawton, T. J.; Sykes, E. C. H.; Gellman, A. J. *J. Phys. Chem. C* **2013**, *117*, 7577–7588.

## ■ NOTE ADDED AFTER ASAP PUBLICATION

Reference 1 was incorrect in the version published ASAP May 6, 2013. The corrected version was re-posted on May 13, 2013.